DOI 10.59887/2073-6673.2024.17(1)-3

UDC 551.465

© *V. A. Gorchakov*[1], *A. Y. Dvornikov*[1], *S. M. Gordeeva*[1,2], *V. A. Ryabchenko*[1], *D. V. Sein*[1,3], 2024
© Translation from Russian: *N. V. Mironova*, 2024

[1]Shirshov Institute of Oceanology, Russian Academy of Sciences, 36 Nakhimovsky Prosp., Moscow, 117997, Russia
[2]Russian State Hydrometeorological University, 79 Voronezhskaya Str., St. Petersburg, 192007, Russia
[3]Alfred Wegener Institute, Helmholtz Centre for Polar and Marine Research, 27570, Am Handelshafen 12, Bremerhaven, Germany
*vikfioran@yandex.ru

SPATIAL STRUCTURE OF THE TEMPORARY VARIABILITY OF THE ARCTIC SEAS SURFACE TEMPERATURE

Received 15.09.2023, Revised 09.12.2023, Accepted 02.02.2024

Abstract

Interannual oscillations in the surface temperature of the Arctic Ocean and the North Atlantic with the southern boundary at latitude 55° 25′ N between 1949 and 2007 are investigated based on the MPIOM (Max Planck Institute Ocean Model) solution. It is a free surface ocean model based on primitive equations in the Boussinesq and incompressibility approximations. High-resolution spectra were estimated via fast Fourier transform with a maximum resolution (Welch's method). Factor analysis method, which makes it possible to identify areas with highly correlated oscillations and reduce the study of the characteristics in question to their analysis in local points, is used to minimize the significant amount of the initial information about monthly average sea surface temperature fields. Analysis of the main factors made it possible to identify 10 areas with quasi-synchronous variability of temperature anomalies by including the points correlated with relevant factors with correlation exceeding 0.6. Spectral structure compliance classification revealed that the areas of the Chukchi Sea, the Hudson Bay, the Irminger Sea, and the Labrador Sea have oscillation peak similarities for the periods of 5–6 years and 8–9 years. Central and western areas of the Norwegian Sea, the area affected by the North Atlantic Current, the eastern part of the Norwegian Sea, and some areas of the Kara Sea have similar spectral structure defined by the peaks at the 11-year and 6-year periods. The Baffin Bay with two main peaks at the 16-year and 5–6-year periods, and the central and the western parts of the Barents Sea, where oscillations are similar to the ones in the Chukchi Sea at short periods, and to the ones in the south-eastern part of the Barents Sea and in the eastern part of the Norwegian Sea at 7–8-year periods, stand out significantly. In some cases, spectrum peaks in different areas appear shifted and attenuated, so presumably the frequency characteristics of the temperature signal change as it moves across the water area.

Keywords: Arctic Ocean, modeling, fast Fourier transform (FFT), Welch's method, temperature oscillation, factor analysis, cluster analysis, spectral structure

УДК 551.465

© *В. А. Горчаков*[1], *А. Ю. Дворников*[1], *С. М. Гордеева*[1,2], *В. А. Рябченко*[1], *Д. В. Сеин*[1,3], 2024
© Перевод с русского: *Н. В. Миронова*, 2024

[1]Институт океанологии им. П.П. Ширшова РАН, 117997, Москва, Нахимовский пр., д. 36
[2]Российский государственный гидрометеорологический университет, 192007, Воронежская ул., д. 79, Санкт-Петербург
[3]Институт Альфреда Вегенера, Центр полярных и морских исследований имени Гельмгольца, 27570, Бремерхафен, Ам Хандельсхафен 12., Германия
*vikfioran@yandex.ru

ПРОСТРАНСТВЕННАЯ СТРУКТУРА ВРЕМЕННОЙ ИЗМЕНЧИВОСТИ ТЕМПЕРАТУРЫ ПОВЕРХНОСТИ АРКТИЧЕСКИХ МОРЕЙ

Статья поступила в редакцию 15.09.2023, после доработки 09.12.2023, принята в печать 02.02.2024

Аннотация

На основе решения модели MPIOM (Max Planck Institute Ocean Model), представляющей собой модель океана со свободной поверхностью, основанную на примитивных уравнениях в приближениях Буссинеска и несжимаемости, за период 1949–2007 гг. исследуются межгодовые колебания температуры поверхности Северного

Ссылка для цитирования: *Горчаков В.А.*, *Дворников А.Ю.*, *Гордеева С.М.*, *Рябченко В.А.*, *Сеин Д.В.* Пространственная структура временной изменчивости температуры поверхности арктических морей // Фундаментальная и прикладная гидрофизика. 2024. Т. 17, № 1. С. 39–51. doi:10.59887/2073-6673.2024.17(1)-3
For citation: *Gorchakov V.A.*, *Dvornikov A.Y.*, *Gordeeva S.M.*, *Ryabchenko V.A.*, *Sein D.V.* Spatial Structure of the Temporary Variability of the Arctic Seas Surface Temperature. *Fundamental and Applied Hydrophysics*. 2024, 17, 1, 39–51. doi:10.59887/2073-6673.2024.17(1)-3

Ледовитого океана и Северной Атлантики с южной границей на широте 55,25°с.ш. Спектры высокого разрешения оценивались методом быстрого преобразования Фурье с максимальным разрешением (метод Велча). Для «сжатия» большого объема исходной информации полей среднемесячных значений температуры поверхности моря используется метод факторного анализа, позволяющий выделить районы с высоко коррелированными колебаниями и свести исследование рассматриваемых характеристик к их анализу в локальных точках. Анализ главных факторов позволил выявить 10 районов с квазисинхронной изменчивостью аномалий температуры путем отнесения к ним точек, имеющих превышающую 0,6 корреляцию с соответствующими факторами. Классификация по соответствию спектральной структуры показала, что районы Чукотское море, Гудзонов залив, моря Ирмингера и Лабрадор имеют совпадения в пиках на периодах колебаний 5–6 лет и 8–9 лет. Схожую спектральную структуру, определяемую пиками на периодах 6 и 11 лет, имеют районы центральной и западной части Норвежского моря, влияния Северо-Атлантического течения, восточная часть Норвежского моря и участки Карского моря. Особняком выделяются Баффинов залив, имеющий два основных пика – на периодах 16 и 5–6 лет, и центральная и западная часть Баренцева моря, где колебания на малых периодах совпадают с колебаниями в Чукотском море, а на периодах 7–8 лет – с колебаниями в юго-восточной части Баренцева моря и восточной части Норвежского моря. В некоторых случаях пики спектров в разных районах проявляются со смещением и ослаблением, т.е. можно предположить, что при переносе температурного сигнала по акватории меняются и его частотные характеристики.

Ключевые слова: Северный Ледовитый океан, моделирование, быстрое преобразования Фурье, метод Велча, колебания температуры, факторный анализ, кластерный анализ, спектральная структура

1. Introduction

The interannual variability of climatic factors in the Arctic Ocean, such as temperature and ice cover area, shows significant differences in the oscillation periods identified in different areas. Thus, according to [1], the results of the data processing from the observations in Kola Meridian section make it possible to identify interannual oscillations with the periods of 4–5, 8–10, 12–13, and 15–17 years. At the same time, in the interannual variability of water temperature in the Barents Sea, studied using PINRO data in [2], periods of 6.2, 18.6 and 55.8 years were identified. According to [3], in the area of the North-European Basin, the atmosphere and ocean circulation periodicity of about 7–8 years was identified, which is formed as a result of the interaction between the atmosphere, ocean and ice in the system of the North Atlantic and the Arctic Ocean. Weak fluctuations in climate characteristics with the periods of 2–3, 10–12, and 20 years were also identified. A 7.7-year period fluctuation in the water temperature and surface atmospheric pressure oscillations in the North Atlantic has been identified [4]. Cycles with the periods of 2.5, 5.1, 8.7, 12.3, and 36.7 years were identified in the air temperature variability at Svalbard meteorological station in Spitsbergen [5]. A special feature of the Barents and Kara Seas area is the uneven change in the water temperature and ice cover area. Thus, in [6] it is shown that the ice cover area of the Arctic Ocean between 1978 and 2018 has significant interannual variability, which is primarily determined by the changes in the influx of warm Atlantic water from the North-European Basin. It also has an important trend leading to the rise of water temperature and significant reduction of the ice cover [7]. However, a decrease in the warm water advection and, accordingly, a decrease in water temperature in the Barents Sea have been observed since 2016 [8]. In work [9], in the White Sea area, temperature oscillations were identified for the periods close to 3, 8, and 14 years, associated with El Niño – Global Atmospheric Oscillation, North Atlantic Oscillation, and the changes in the North Atlantic Current, respectively, while in the Barents Sea area, a quasi-15-year temperature oscillation was revealed, which is caused by the heat advection from the North Atlantic [10].

The above studies based on observational data are not able to describe the spatiotemporal structure of the Arctic Ocean interannual oscillations due to the small number of and limited access to the data of long-term observations at the local geographic points or sections.

Currently, attempts are being made to overcome this drawback by using mathematical models of ocean circulation. For example, in work [11], where seasonal and interannual variations of advective heat fluxes in the ocean and atmosphere of the Barents Sea area between 1993 and 2012 were studied based on the results of the MIT regional eddy-resolving ocean model and the ERA-Interim atmospheric reanalysis. The wavelet analysis and singular spectral analysis methods used by the authors made it possible to identify the cycles with 2–4-year and 5–8-year periods, which are in good agreement with the observational results. In work [12], mathematical methods, on the contrary, are used to study the causes and mechanisms regulating the intensity and duration of empirically identified Arctic circulation regimes, and to explain well-defined decadal changes in the area

between 1948 and 1996 and in the period of the obvious termination of the circulation regimes quasi-decadal cycle after 1996. In work [13], using two models of different resolutions (a global one, using the ROM model complex (regionally coupled atmosphere-ocean-sea ice-marine biogeochemistry model) [14], and a regional one, MITgcm – Massachusetts Institute of Technology general circulation model [15]), a solution was obtained that made it possible to identify the ranges of the 3 main oscillation carrier frequencies, corresponding to the periods of 1.0–3.6, 3.9–5.8, and 6.3–10.5 years.

Thus, it is obvious that in different regions of the Arctic Ocean climatic factors have strong variability, because they are defined by both global and regional mechanisms with a significant number of feedbacks, and many features of interconnections remain understudied [16]. However, the influence of feedbacks and their intensity can be investigated by analyzing time series data characterizing climate fluctuations in the Arctic Ocean.

The purpose of this work is to identify the main interannual water temperature oscillations and to assess water spatial structure in the Arctic Ocean and the North Atlantic up to the southern boundary of the basin, located at latitude 55° 25′ N, based on average monthly water temperature data obtained as a result of calculations using the regional Earth system model ROM (regionally coupled atmosphere-ocean-sea ice-marine biogeochemistry model) [14]. To analyze long-period oscillations of the Arctic Ocean, model-averaged monthly averages were used, interpolated onto a uniform grid with a step of 0.5° in latitude and longitude. High-resolution spectra were estimated using fast Fourier transform method with maximum resolution, which increases spectral resolution and thus enables more accurate detection of spectral density peaks at periods, which are not multiples of the total length of the original record.

2. Methods and Approaches

2.1. Description of the models and methods used

The analysis is based on average monthly water temperature data obtained from simulations using the ROM [14]. The oceanic component of the ROM is the coupled (ocean-sea ice) MPIOM (Max Planck Institute Ocean Model) [17]. MPIOM is a free surface ocean model based on primitive equations in the Boussinesq and incompressibility approximations. The model is implemented on an orthogonal curvilinear C-grid [18]. The ocean MPIOM grid covers the entire World Ocean and has high resolution in the North Atlantic and the North-European shelf. The horizontal resolution gradually changes from a minimum of 5 km in the North Sea to a maximum of 220 km in the Antarctic. Vertically, the MPIOM grid has 30 z-levels. Atmospheric data from the NCEP/NCAR reanalysis [19] for the period between 1949 and 2007 are used as boundary conditions on the sea surface. In z-coordinate climate models that explicitly reproduce tidal dynamics, such as MPIOM, the top layer is selected considering the maximum possible tidal height. Thus, the thickness of the upper layer in this experiment was 16 m, and the depth to which the sea surface temperature (SST) is tied was 8 m. In other words, the model SST is the temperature of the upper 16-meter layer of the model. This temperature is used for comparison with the data from observations on the sea surface. Therefore, everywhere including the areas covered with ice, the SST is the water temperature in the specified upper layer.

The tidal influence on the ocean in the model is obtained from the total ephemeris luni-solar tidal potential [20]. Further details on the model settings, as well as comparison of calculation results with observations are presented in [14, 21].

To analyze long-period oscillations of the Arctic Ocean, model monthly averages are used, interpolated onto a uniform grid with a step of 0.5° in latitude and longitude. At the same time, the southern boundary of the basin is located at latitude 55° 25′ N. Thus, the initial data are matrices of 80 × 720 values, from 55° 25′ N to 89° 75′ N and from 179° 75′ W to 179° 75′ E, at 708 points of the time series from January 1949 to December 2007.

High-resolution spectra were estimated via fast Fourier transform with a maximum resolution. This approach is based on the following idea. Each observation record of any hydrological characteristic, even one continuously varying in time, has a finite length and finite time resolution and cannot be represented by a Fourier integral S(f) in which f is a continuously varying frequency. It only can be represented by a finite series of Fourier coefficients S(f), where f is from a discrete sequence of frequencies corresponding to harmonics that are multiples of the total record length. As a result, the Fourier amplitude of harmonics that are not multiples of the total record length may be underestimated if this amplitude differs significantly from the ones of nearby har-

monics. To eliminate this effect, you can use the Welch's method proposed in [22], which consists in repeated calculating the periodograms that remain after successive reduction of the initial record. Subsequently, all such periodograms are combined and, if the periods coincide, are averaged. This increases the spectral resolution and thus makes it possible to more accurately locate spectral density peaks at periods that are not a multiple of the original record total length.

Maximum resolution spectra are built by successively reducing the time series length to the half of its original length, since this produces the most continuous estimates of spectral density for all frequencies. Spectra are evaluated first for the series of length N: (1,..., N); then for 2 series of length N-1: (1,..., N-1) and (2,..., N); then for 3 series of length N-2: (1,..., N-2), (2,..., N-1), and (3,..., N), etc. up to N/2 series of length N/2: (1,..., N/2), (2,..., N/2+1), ..., (N/2,..., N). Then all the obtained spectra are combined into one by ordering them by frequencies and averaging when the frequencies coincide [23].

Using this method, spectra are estimated not only for the total record length, but also for gradually reduced time series, which is followed by combining all obtained periodograms.

2.2. Selection of representative points

Studying the temporal variability of hydrological characteristics throughout the entire Arctic Ocean requires processing a large amount of information. To minimize this amount, the work uses a multivariate statistics method such as factor analysis [24], which makes it possible to identify areas with highly correlated oscillations and reduce the study of the characteristics under consideration to their analysis at local points reflecting these areas. The method was applied to the monthly mean SST fields obtained from the ROM model.

Seasonal variability was removed from each point of the SST field by subtracting the long-term average annual variation. The obtained SST anomalies (SSTA) were assessed by the value of the standard deviation. Points with standard deviation less than 0.001 °C (in the central zone of the Arctic Ocean) were excluded. For the remaining monthly SSTA values for 59 years (from 1949 to 2007) an analysis of the main factors was carried out at 708 points. The convergence of the matrix decomposition presented in Table 1 for the first 10 factors demonstrates their total variance equal to 52.4 % of the entire matrix variance.

Variance redistribution by the second rotation of the factor axes made it possible to identify the areas with quasi-synchronous SST variability by assigning to them points that have a correlation with the corresponding factors, exceeding 0.6. As a result, the basin was divided into 10 areas (Fig. 1), where the SSTAs can be con-

Table 1

Convergence of factor decomposition before the second rotation for monthly SSTA at 708 points of the Arctic Ocean for the period between 1949 and 2007

Factor number	Eigenvalue	Dispersion,%	Cumulative dispersion,%
1	150.9	21.3	21.3
2	54.7	7.7	29.0
3	35.1	5.0	33.9
4	28.7	4.1	38.0
5	21.9	3.1	41.1
6	21.4	3.0	44.1
7	16.4	2.3	46.4
8	14.8	2.1	48.5
9	14.4	2.0	50.5
10	13.3	1.9	52.4

sidered highly intercorrelated. Points in the central and eastern parts of the Arctic Ocean have SSTA standard deviation less than 0.001 °C due to the presence of sea ice, so these areas were excluded from the analysis. Remember that the selected 10 areas represent only 52 % of the total SSTA variance and characterize large-scale fields and oscillations. The points not included in any of the areas reflect the remaining 48 % (2,294 factors) – smaller and more local oscillations. They were not considered.

As can be seen from the Fig. 1, the areas almost coincide with their geographical features (Table 2).

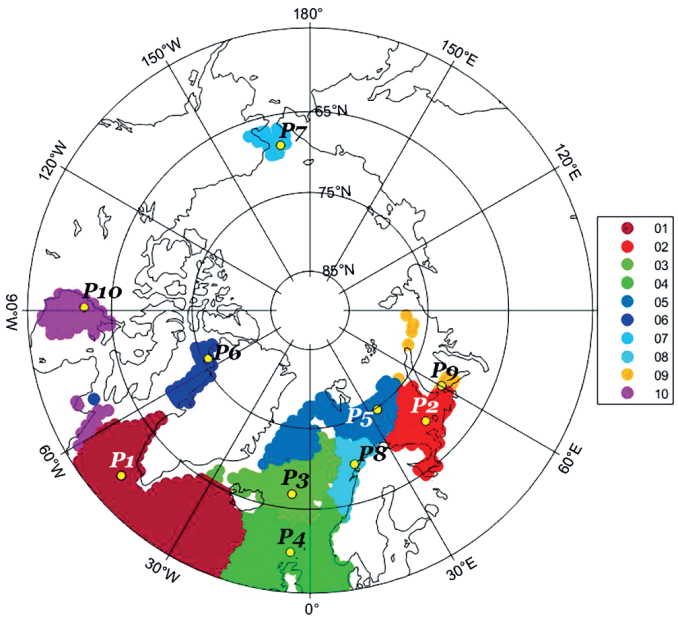

Fig. 1. Factor analysis results: areas 1–10 with quasi-synchronous interannual SST variability for the period between 1949 and 2007 according to the ROM model. The positions of the points under study (P1–P10) are indicated with yellow dots

Table 2

Accordance of the selected areas to their geographical features

Area number	Geographic reference	Abbreviation
1	Irminger Sea and Labrador Sea	IL
2	South-eastern part of the Barents Sea	SEB
3	Central and western Norwegian Sea	WNS
4	Area of influence of the North Atlantic Current 55–65°N	NA
5	Central and western Barents Sea	CWB
6	Baffin Bay	BB
7	Chukchi Sea	ChS
8	Eastern Norwegian Sea	ENS
9	Parts of the Kara Sea	KS
10	Hudson Bay	HB

3. Results

3.1. Water temperature oscillations at the stations in the Kola Meridian section

As was shown in [13], at the points of the Kola Meridian section, the amplitudes of seasonal and interannual oscillations are of the same order of magnitude. Thus, the contribution of interannual temperature oscillations to the overall pattern of oscillations turns out to be significant.

The initial comparison of the results was performed based on the data from the Kola Meridian section [25]. Available data at the stations of the Kola Meridian section (33° 50′ E) were spatially averaged for stations 3–7, point K3–7 was assigned to station 5 (71° 50′ N). Calculations were made both on the basis of fast Fourier transform (FFT) and the Welch's method. Before proceeding to the result analysis, it is important to note, firstly, that the calculation based on the Welch's method gives an unnecessarily large number of small peaks, which complicate the analysis. To eliminate this feature of the solution and smooth the obtained spectrum, a Hamming filter with a window of 31 was applied to it [26]. Secondly, since the length of the original series does not exceed 59 years, it is reasonable to consider only interannual oscillations with periods in the range of no more than 20 years. The calculation results based on FFT and the Welch's method with subsequent Hamming filtering are presented in Fig. 2.

In the existing results of data processing from the observations in the Kola Meridian section, presented, for example, in [1], the periods of 4–5, 8–10, 12–13, and 15–17 years are distinguished in interannual oscillations. In the spectrograms obtained from processing longer series of data from the same section (Fig. 2), oscillations in the ranges of 2–3, 4–5, 6.5–7.5, and 12 years are distinguished. Oscillations at the periods of 8–10 years are not distinguished in our calculation. Moreover, a comparison of the results obtained by different methods shows that the FFT gives a spectrum picture with a smaller number of peaks compared to the spectrogram obtained using the Welch's method. Thus, in the FFT spectrogram there is no peak at the period of 12 years, and most of the FFT peaks that coincide in both calculations are somewhat shifted towards longer periods. A more detailed analysis of the spectra at the frequencies of 1–2 years generally confirms the general pattern identified for the FFT and Welch's method spectrograms, and also demonstrates a slightly better reproduction of Chandler oscillations with a period of 14 months in the case of using the Welch's method.

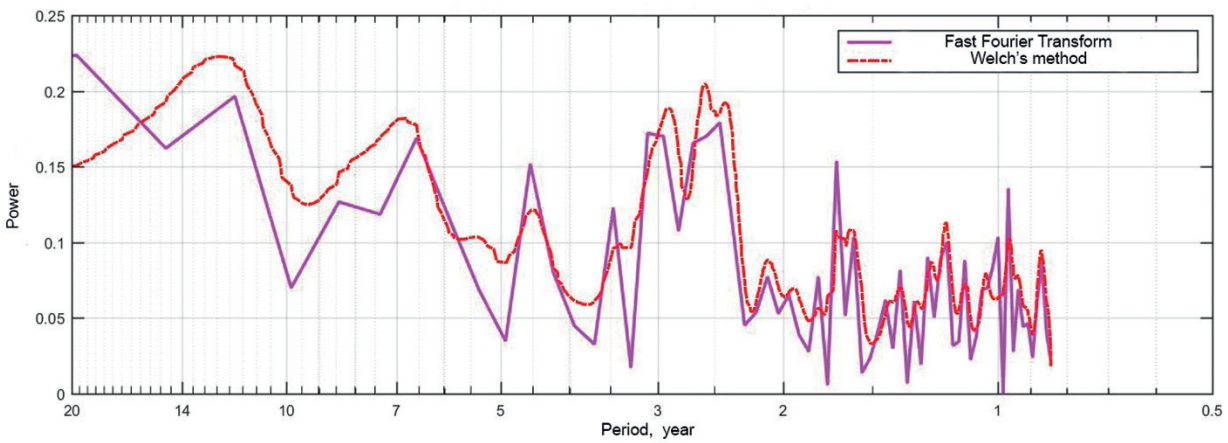

Fig. 2. Oscillation spectra of temperature anomalies on the K3–7 station of the «Kola» section, obtained via fast Fourier transform (the violet line) and the Welch's method (the red dotted line) for 0.5–20-year periods

Thus, it can be argued that spectrograms calculated using the Welch's method provide a more detailed and better picture than those calculated using standard FFT.

3.2. Analysis of oscillations in various areas of the studied part of the ocean

As shown in Section 2.2, in the studied part of the ocean, 10 areas with quasi-synchronous SST variability can be identified. Spectral analysis of SSTA time series using the Welch's method was performed at one point in each area, which had the maximum correlation with the corresponding factor (points are shown as asterisks in Fig. 1). The spectra calculated for all 10 areas, combined on one diagram, are presented in Fig. 3.

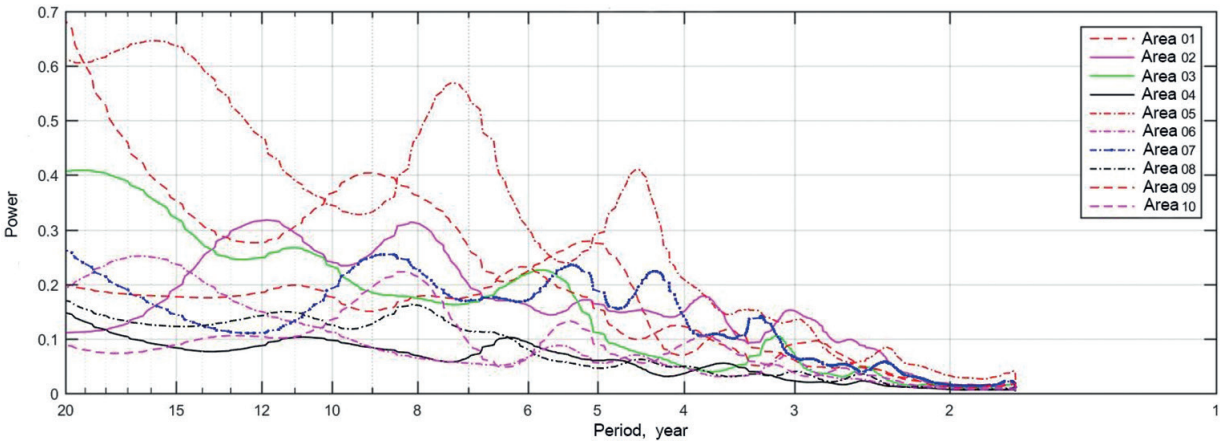

Fig. 3. Oscillation spectra of temperature anomalies, obtained via Welch's method at the 1–20-year period in each of 10 areas

As you can see, it is quite difficult to identify oscillations with periods common to all areas. Therefore, to generalize the picture based on the spectrum peaks, oscillations were identified in different period intervals, presented in Table 3. According to the table, the 'noisiest' areas with the largest number of spectral components are areas 2, 5 and 7 (the southeastern part of the Barents Sea, central and western parts of the Barents Sea, the Chukchi Sea, respectively). This can be explained by the fact that the Barents and Chukchi Seas located on the shelf are characterized by strong transformation of waters, especially in the surface layer. The frequency structure throughout the Arctic zone is dominated by oscillation periods of 5–6 years, 3–3.3 years and 8–9 years.

To identify groups of areas that have oscillations of close periods using Table 3, cluster analysis was performed with the Hamming metric. The results are presented in Fig. 4.

Table 3

Peaks in the given period intervals

Area number and its abbreviated name	Period, years										Sum of cases
	16	12	11	8–9	7	5–6	4–5	3–4	3–3.3	2.3	
1 IL	–	–	–	+	–	+	–	+	–	–	3
2 SEB	–	+	–	+	–	+	–	+	+	–	5
3 WNS	–	–	+	–	–	+	–	–	+	–	3
4 NA	–	–	+	–	–	–	–	+	–	–	2
5 CWB	+	–	–	–	+	–	+	–	+	+	5
6 BB	+	–	–	–	–	+	–	–	–	–	2
7 ChS	–	–	–	+	–	+	+	–	+	+	5
8 ENS	–	–	+	+	–	–	–	–	–	–	2
9 KS	–	–	+	–	–	+	+	–	+	–	4
10 HB	–	–	–	+	–	+	–	+	+	–	4
Sum of cases	2	1	4	5	1	7	3	4	6	2	

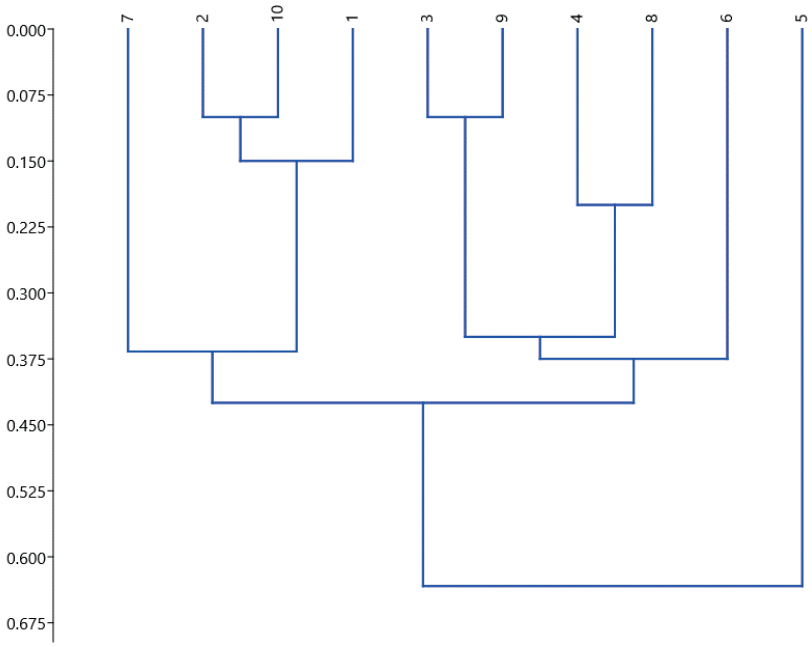

Fig. 4. Dendrogram of the spectral structure compliance classification for SST areas for the period 1949–2007 according to the ROM model. The vertical axis shows the probability of non-compliance

Spectral structure compliance classification revealed that areas 7, 10, 1, and 2 (the Chukchi Sea, the Hudson Bay, the Irminger Sea, the Labrador Sea, the southeastern part of the Barents Sea) are similar, primarily by the coincidence of oscillations at the periods of 8–9 years and 5–6 years (Fig. 5a). Areas 3, 4, 8, and 9 (central and western parts of the Norwegian Sea, the area affected by the North Atlantic Current at 55–65° N, the eastern part of the Norwegian Sea, and some areas of the Kara Sea) have a similar spectral structure, determined by the periods of 11 and 6 years (Fig. 5b). While the first group of areas is characterized by cold surface waters and their transformation associated with further cooling and interaction with the ice cover, the second group of areas is obviously associated with Atlantic waters entering the Arctic Ocean from the south.

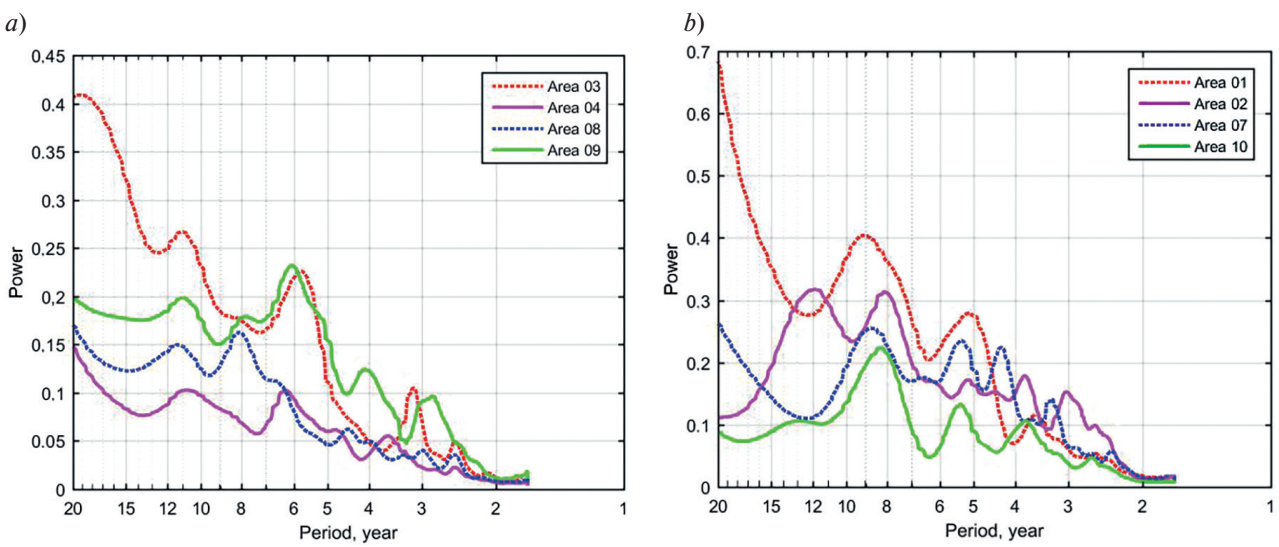

Fig. 5. Fin p. 47

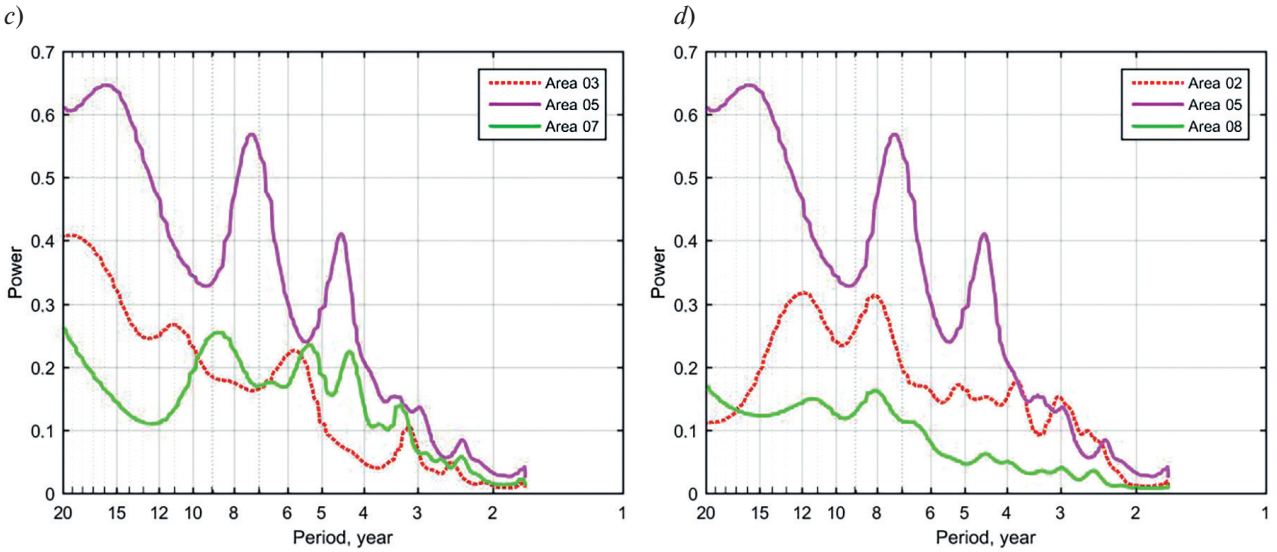

Fig. 5. Oscillation spectra of temperature anomalies, obtained via Welch's method in 1–20-year periods for areas 1 (the Irminger Sea and the Labrador Sea), 2 (south-east of the Barents Sea), 7 (the Chukchi Sea), and 10 (the Hudson Bay) (*a*); areas 3 (central and western parts of the Norwegian Sea), 4 (the area affected by the North Atlantic Current), 8 (the eastern part of the Norwegian Sea), and 9 (The Kara Sea) (*b*); areas 2 (south-east of the Barents Sea), 5 (central and western parts of the Barents Sea), and 8 (the eastern part of the Norwegian Sea) (*c*); areas 3 (central and western parts of the Norwegian Sea), 5 (central and western parts of the Barents Sea), and 7 (the Chukchi Sea) (*d*).

The Baffin Bay area (area 6) stands out: it has two main peaks – at the long period of 16 years and at the 5–6-year period common to the Arctic Ocean.

Area 5 (central and western parts of the Barents Sea) also stands out from the entire array. At short periods (2.3 years, 3.3 years, 4.5 years), SST oscillations there almost coincide with oscillations in the Chukchi Sea area (area 7) (Fig. 5c), and at the periods of 7–8 years – with oscillations in areas 2 and 8 (the southeastern part of the Barents Sea, the eastern part of the Norwegian Sea) (Fig. 5d). A special feature of this area is the presence of a highly mobile ice boundary, which is not the case in other areas. Therefore, the spectral structure of this water area differs from the areas that do not have this feature.

However, it can also be seen that in some cases the spectrum peaks appear shifted and attenuated (Fig. 6).

For example, the original relatively long-period oscillation (with a period of 3.5 years) in the Irminger and Labrador Seas (area 1) appears with a shorter period of 3.2 years in the Norwegian Sea (area 3), and the oscillation with an initial period of 2.6 years has a period

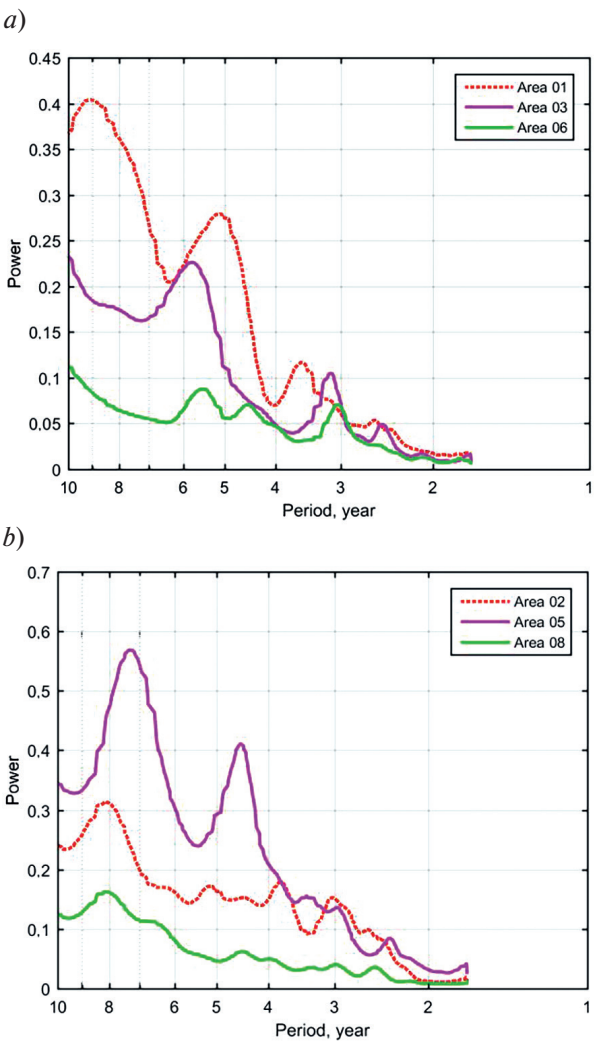

Fig. 6. Oscillation spectra of temperature anomalies, obtained via Welch's method in 1–10-year periods for areas 1 (the Irminger Sea and the Labrador Sea), 3 (central and western parts of the Norwegian Sea), 6 (The Baffin Bay) (*a*), and for areas 2 (the south-eastern part of the Barents Sea), 5 (central and western parts of the Barents Sea), and 8 (the western part of the Norwegian Sea) (*b*)

of 2.5 years. In the Baffin Sea (area 6), the first oscillation is even shorter, with a period of 3 years (Fig. 6a). Another oscillation in the central and western parts of the Barents Sea (area 5) with a period of 7.2 years extends to a period of 7.9 years in the south-eastern part of the Barents Sea (area 2), and in the eastern part of the Norwegian Sea it is already observed with a period of 8.1 years (area 8) (Fig. 6b). Thus, we can put forward a hypothesis that the frequency characteristics of the temperature signal change as it moves across the water area. However, this hypothesis requires additional research.

4. Conclusions

1. Comparison of the results obtained using the standard FFT and the Welch's method, performed on the data from the Kola Meridian section, demonstrates that the FFT gives a spectrum picture with a smaller number of peaks, compared to the spectrogram obtained using the Welch's method. Thus, in the FFT spectrogram there is no peak at a period of 12 years, and most of the FFT peaks that coincide in both calculations are somewhat shifted towards longer periods.

2. In the water area under consideration, 10 areas with quasi-synchronous SST variability can be identified. It turned out that it is quite difficult to identify oscillations with periods common to all areas, but it is possible to identify areas with coinciding oscillations of different periods. The 'noisiest' areas with the largest number of spectral components are areas 2, 5 and 7 (the southeastern part of the Barents Sea, central and western parts of the Barents Sea, the Chukchi Sea, respectively). The frequency structure throughout the Arctic zone is dominated by oscillation periods of 5–6 years, 3–3.3 years and 8–9 years.

3. Spectral structure compliance classification revealed that areas 7, 10, 1, and 2 (the Chukchi Sea, the Hudson Bay, the Irminger Sea, the Labrador Sea, the southeastern part of the Barents Sea) are similar, primarily by the coincidence of oscillations for the periods of 8–9 years and 5–6 years. Areas 3, 4, 8, and 9 (central and western parts of the Norwegian Sea, the area affected by the North Atlantic Current at 55–65° N, the eastern part of the Norwegian Sea, and some areas of the Kara Sea) have a similar spectral structure, determined by the periods of 11 and 6 years.

4. Particularly notable are the Baffin Bay area (area 6), which has two main peaks – at the period of 16 years and at the 5–6-year period common to the Arctic Ocean, and the area of the central and western parts of the Barents Sea (area 6), in which SST oscillations at short periods (2.3 years, 3.3 years, 4.5 years) nearly coincide with oscillations in the Chukchi Sea area (area 7), and oscillations at the periods of 7–8 years nearly coincide with oscillations in areas 2 and 8 (the southeastern part of the Barents Sea, the eastern part of the Norwegian Sea).

5. In some cases, spectrum peaks appear shifted and attenuated. Thus, we can put forward a hypothesis that the frequency characteristics of the temperature signal change as it moves across the water area. However, this hypothesis requires additional research.

Funding

The work was carried out within the theme of the state assignments No FMWE-2024–0028.

References

1. *Bochkov Yu.A.* Forecast of water temperature in the Barents Sea for 1965–1970. *Proceeding of the PINRO Academic Council Session on the Results of Research in 1964*, release IV, 64–79 (in Russian).
2. *Yndestad H.*, *Turrell W.R.*, *Ozhigin V.* Lunar nodal tide effects on variability of sea level, temperature, and salinity in the Faroe-Shetland Channel and the Barents Sea. *Deep-Sea Research Part I*: *Oceanographic Research Papers*. 2008, 55, 10, 1201–1217. doi:10.1016/j.dsr.2008.06.003
3. *Smirnov N.P.*, *Vorobyov V.N.*, *Drozdov V.V.* Cyclonic center of atmosphere and ocean action in North Atlantic. *Proceeding of RSHU*. 2010, 15, 117–134 (in Russian).
4. *Da Costa E.*, *De Verdiere C.* The 7.7-year North Atlantic Oscillation. *Quarterly Journal of the Royal Meteorological Society*. 2002, 128, 797–817.
5. *Humlum O.*, *Solheim J.-E.*, *Stordahl K.* Spectral analysis of the Svalbard temperature record 1912–2010. *Advances in Meteorology*. 2011, Article ID175296, 14 p. doi:10.1155/2011/175296
6. *Yulin A.V.*, *Vyazigina N.A.*, *E.S. Egorova E.S.* Interannual and seasonal variability of Arctic Sea ice extent according to satellite observations. *Russian Arctic*. 2019, 7, 28–40. dot:10.24411/2658-4255-2019-10073

7. IPCC, 2014: Climate Change 2014: Synthesis Report. Contribution of working groups I, II and III to the Fifth Assessment Report of the intergovernmental panel on climate change [CoreWriting Team, R.K. Pachauri and L.A. Meyer (eds.)]. IPCC: Geneva, Switzerland, 2014. 151 p.
8. *Jelmert A.*, *Sandø A.B.*, *Frie A.K.* et al. Status for miljøet i Barentshavet. Rapport fra Overvåkingsgruppen 2020. *Havforskningsinstituttet.* 2020. Electronic resource. URL: https://www.hi.no/hi/nettrapporter/rapport-fra-havforskningen-2020-13 (date of access: 09.06.2020).
9. *Serykh I.V.*, *Kostianoy A.G.*, *Lebedev S.A.*, *Kostianaia E.A.* On the transition of temperature regime of the White Sea region to a new phase state. *Fundamental and Applied Hydrophysics*. 2022, 15, 1, 98–111. doi:10.59887/fpg/k9x4-p8fz-5kz6
10. *Serykh I.V.*, *Kostianoy A.G.* On climatic changes in the temperature of the Barents Sea and their possible causes. *The Barents Sea System* / edited by the Academician Lisitsin. *M.*, *GEOS*, 2021. 672 p. (in Russian).
11. *Bashmachnikov I.L.*, *Yurova A.U.*, *Bobylev L.P.*, *Vesman A.V.* Seasonal and interannual variations of the heat fluxes in the Barents Sea region. *Izvestiya, Atmospheric and Oceanic Physics*. 2018, 54, 2, 213–222. doi:10.1134/S0001433818020032
12. *Proshutinsky A.*, *Dukhovskoy D.*, *Timmermans M.L.*, *Krishfield R.*, *Bamber J.L.* Arctic circulation regimes. *Philosophical Transactions of the Royal Society A*: *Mathematical*, *Physical and Engineering Sciences*, 2015, 373(2052), 20140160. doi:10.1098/rsta.2014.0160
13. *Gorchakov V.A.*, *Dvornikov A.Y.*, *Gordeeva S.M.*, *Ryabchenko V.A.* Spatial variability of interannual temperature oscillations in the Barents Sea and the Kara Sea according to simulation results. *Fundamental and Applied Hydrophysics*. 2020, 13, 4, 50–65. doi:10.7868/S207366732004005X (in Russian).
14. *Sein D.V.*, *Mikolajewicz U.*, *Groger M.*, *Fast I.*, *Cabos W.*, *Pinto J.G.*, *Hagemann S.*, *Semmler T.*, *Izquierdo A.*, *Jacob D.* Regionally coupled atmosphere-ocean-sea ice-marine biogeochemistry model ROM: 1. Description and validation. *Journal of Advances in Modeling Earth Systems*. 2015, 7, 268–304. doi:10.1002/2014MS000357
15. *Marshall J.*, *Adcroft A.*, *Hill C.*, *Perelman L.*, *Heisey C.* A finite-volume, incompressible navier-stokes model for studies of the ocean on parallel computers. *Journal of Geophysical Research Atmospheres*. 1997, 102(C3), 5753–5766.
16. *Sherstyukov B.G.* Climatic conditions of the Arctic and new approaches to forecasting climate change. *Arctic and North*. 2016, 24, 39–67.
17. *Marsland S. J.*, *Haak H.*, *Jungclaus J.H.*, *Latif M.*, *Roske F.* The Max-Planck-Institute global ocean/sea ice model with orthogonal curvilinear coordinates. *Ocean Modelling*. 2003, 5, 91–127. doi:10.1016/S1463-5003(02)00015-X
18. *Arakawa A.*, *Lamb V.R.* Computational design of the basic dynamical processes of the UCLA general circulation model, Methods. *Methods in Computational Physics*: *Advances in Research and Applications*. 1977, 17, 173–265. doi:10.1016/B978-0-12-460817-7.50009-4
19. *Kistler R.* et al. The NCEP/NCAR50 year reanalysis: Monthly-means CD-ROM and documentation. *Bulletin of the American Meteorological Society*. 2001, 82, 247–267.
20. *Thomas M.*, *Sündermann J.*, *Maier-Reimer E.* Consideration of ocean tides in an OGCM and impacts on subseasonal to decadal polar motion excitation. *Geophysical Research Letters*. 2001, 28, 2457–2460. doi:10.1029/2000GL012234
21. *Sein D.V.*, *Gröger M.*, *Cabos W.* et al. Regionally coupled atmosphere-ocean-marine biogeochemistry model ROM: 2. Studying the climate change signal in the North Atlantic and Europe. *Journal of Advances in Modeling Earth Systems*. 2020, 12, e2019MS00164. doi:10.1029/2019MS001646
22. *Welch P.D.* The use of Fast Fourier Transform for the estimation of power spectra: A method based on time averaging over short, modified periodograms. *IEEE Transactions on Audio and Electroacoustics*, 1967. AU-15 (2): 70–73.
23. *Serykh I.V.*, *Sonechkin D.M.* Nonchaotic and globally synchronized short-term climatic variations and their origin. *Theoretical and Applied Climatology*. 2019, 137, 3–4, 2639–2656. doi:10.1007/s00704-018-02761-0
24. *Rummel R.J.* Applied factor analysis:1st edition. *Evanston*, *USA*, *Northwestern University Press*, 1988. 617 p.
25. *Karsakov A.L.* Oceanographic studies at the Kola Meridian Section in the Barents Sea for the period 1900–2008. *Murmansk*, *PINRO Publishing*, 2009. 139 p. (in Russian).
26. *Hamming R.W.* The art of doing science and engineering: Learning to learn. *Amsterdam*, *Netherlands*, *Gordon and Breach Science Publishers*, 1997. 227 p.

Литература

1. *Бочков Ю.А.* Прогноз температуры воды в Баренцевом море на 1965–1970 годы // Материалы сессии ученого совета ПИНРО по результатам исследований в 1964 г. Вып. IV. С. 64–79.
2. *Yndestad H.*, *Turrell W.R.*, *Ozhigin V.* Lunar nodal tide effects on variability of sea level, temperature, and salinity in the Faroe-Shetland Channel and the Barents Sea // Deep-Sea Research Part I: Oceanographic Research Papers. 2008. Vol. 55, N 10. P. 1201–1217. doi:10.1016/j.dsr.2008.06.003

3. *Смирнов Н.П.*, *Воробьев В.Н.*, *Дроздов В.В.* Циклонический центр действия атмосферы и океана в Северной Атлантике // Ученые записки РГГМУ. 2010. № 15. С. 117–134.
4. *Da Costa E.*, *De Verdiere C.* The 7.7-year North Atlantic oscillation // Quarterly Journal of the Royal Meteorological Society. 2002. Vol. 128, N 581. P. 797–817. doi:10.1256/0035900021643692
5. *Humlum O.*, *Solheim J.-E.*, *Stordahl K.* Spectral analysis of the svalbard temperature record 1912–2010 // Advances in Meteorology. 2011. Article ID175296. 14 p. doi:10.1155/2011/175296
6. *Юлин А.В.*, *Вязигина Н.А.*, *Егорова Е.С.* Межгодовая и сезонная изменчивость площади льдов в Северном Ледовитом океане по данным спутниковых наблюдений // Российская Арктика. 2019. № 7. С. 28–40. doi:10.24411/2658-4255-2019-10073
7. IPCC, 2014: Climate Change 2014: Synthesis Report. Contribution of Working Groups I, II and III to the Fifth Assessment Report of the Intergovernmental Panel on Climate Change [CoreWriting Team, R.K. Pachauri and L.A. Meyer (eds.)]. IPCC: Geneva, Switzerland, 2014. 151 p.
8. *Jelmert A.*, *Sandø A.B.*, *Frie A.K.* et al. Status for miljøet i Barentshavet. Rapport fra Overvåkingsgruppen 2020 // Havforskningsinstituttet. 2020. [электронный ресурс]. URL: https://www.hi.no/hi/nettrapporter/rapport-fra-havforskningen-2020–13 (дата обращения: 09.06.2020).
9. *Серых И.В.*, *Костяной А.Г.*, *Лебедев С.А.*, *Костяная Е.А.* О переходе температурного режима региона Белого моря в новое фазовое состояние // Фундаментальная и прикладная гидрофизика. 2022. Т. 15, № 1. С. 98–111. doi:org/10.59887/fpg/k9x4-p8fz-5kz6
10. *Серых И.В.*, *Костяной А.Г.* О климатических изменениях температуры Баренцева моря и их возможных причинах // Система Баренцева моря / под ред. академика А.П. Лисицына. М.: ГЕОС, 2021. 672 с.
11. *Башмачников И.Л.*, *Юрова А.Ю.*, *Бобылев Л.П.*, *Весман А.В.* Сезонная и межгодовая изменчивость потоков тепла в районе Баренцева моря // Известия РАН. Физика атмосферы и океана. 2018. Т. 54, № 2. С. 239–249. doi:10.7868/S0003351518020149
12. *Proshutinsky A.*, *Dukhovskoy D.*, *Timmermans M.L.*, *Krishfield R.*, *Bamber J.L.* Arctic circulation regimes. Philosophical Transactions of the Royal Society A: Mathematical, Physical and Engineering Sciences. 2015. 373(2052). 20140160. doi:10.1098/rsta.2014.0160
13. *Горчаков В.А.*, *Дворников А.Ю.*, *Гордеева С.М.*, *Рябченко В.А.* Пространственная изменчивость межгодовых колебаний температуры Баренцева и Карского морей по результатам моделирования // Фундаментальная и прикладная гидрофизика. 2020. Т. 13, № 4. С. 50–65. doi:10.7868/S207366732004005X
14. *Sein D.V.*, *Mikolajewicz U.*, *Groger M.*, *Fast I.*, *Cabos W.*, *Pinto J.G.*, *Hagemann S.*, *Semmler T.*, *Izquierdo A.*, *Jacob D.* Regionally coupled atmosphere-ocean-sea ice-marine biogeochemistry model ROM: 1. Description and validation // Journal of Advances in Modeling Earth Systems. 2015. Vol. 7, N 1. P. 268–304. doi:10.1002/2014MS000357
15. *Marshall J.*, *Adcroft A.*, *Hill C.*, *Perelman L.*, *Heisey C.* A finite-volume, incompressible navier-stokes model for studies of the ocean on parallel computers // Journal of Geophysical Research Atmospheres. 1997. Vol. 102(C3). P. 5753–5766. dot:10.1029/96JC02775
16. *Шерстюков Б.Г.* Климатические условия Арктики и новые подходы к прогнозу изменения климата // Арктика и Север. 2016. № 24. P. 39–67. doi:10.17238/issn2221-2698.2016.24.39
17. *Marsland S.J.*, *Haak H.*, *Jungclaus J.H.*, *Latif M.*, *Roske F.* The Max-Planck-Institute global ocean/sea ice model with orthogonal curvilinear coordinates // Ocean Modelling. 2003. Vol. 5. P. 91–127. doi:10.1016/S1463-5003(02)00015-X
18. *Arakawa A.*, *Lamb V.R.* Computational design of the basic dynamical processes of the UCLA general circulation model // Methods in Computational Physics: Advances in Research and Applications. 1977. Vol. 17. P. 173–265. doi:10.1016/B978-0-12-460817-7.50009-4
19. *Kistler R.* et al. The NCEP-NCAR50-year reanalysis: Monthly means CD-ROM and documentation // Bulletin of the American Meteorological Society. 2001. Vol. 82, N 2. P. 247–268. doi:10.1175/1520-0477(2001)082<0247: TNNYRM>2.3.CO;2
20. *Thomas M.*, *Sündermann J.*, *Maier-Reimer E.* Consideration of ocean tides in an OGCM and impacts on subseasonal to decadal polar motion excitation // Geophysical Research Letters. 2001. Vol. 28, N 12. P. 2457–2460. doi:10.1029/2000GL012234
21. *Sein D.V., Gröger M., Cabos W. et al.* Regionally coupled atmosphere-ocean-marine biogeochemistry model ROM: 2. Studying the climate change signal in the North Atlantic and Europe // Journal of Advances in Modeling Earth Systems. 2020. Vol. 12. e2019MS00164. doi:10.1029/2019MS001646
22. *Welch P.D.* The use of Fast Fourier Transform for the estimation of power spectra: A method based on time averaging over short, modified periodograms // IEEE Transactions on Audio and Electroacoustics. 1967. AU-15 (2): 70–73.

23. *Serykh I.V.*, *Sonechkin D.M.* Nonchaotic and globally synchronized short-term climatic variations and their origin // Theoretical and Applied Climatology. 2019. Vol. 137. N 3–4. P. 2639–2656. doi:10.1007/s00704-018-02761-0
24. *Rummel R.J.* Applied factor analysis:1st edition. — Evanston, USA: Northwestern University Press, 1988. 617 p.
25. *Карсаков А.Л.* Океанографические исследования на разрезе «Кольский меридиан» в Баренцевом море за период 1900–2008 гг. Мурманск: Изд-во ПИНРО, 2009. 139 с.
26. *Hamming R.W.* The art of doing science and engineering: Learning to learn. Amsterdam, Netherlands, Gordon and Breach Science Publishers, 1997. 227 p.

About the Authors

GORCHAKOV, Viktor A., senior researcher, Cand. Sc. (Phys.-Math.), ORCID ID: 0009-0003-3270-4539, Scopus Author ID: 36892327800, РИНЦ Author ID: 70653, e-mail: vikfioran@yandex.ru

DVORNIKOV, Anton Yu., leading researcher, Cand. Sc. (Phys.-Math.), ORCID ID: 0000-0002-9334-3138, WoS ResearcherID: B-5971–2017, Scopus Author ID: 7006072591, SPIN code: 6863-5988, e-mail: anton.dvornikoff@gmail.com

GORDEEVA, Svetlana M., senior researcher, associate professor, Cand. Sc. (Geogr.), ORCID ID: 0000-0001-9797-5266, WoS ResearcherID H-5890–2013, Scopus Author ID:6506898803, SPIN code: 7836-2105, e-mail: smgordeeva@yandex.ru

RYABCHENKO, Vladimir A., chief researcher, Senior Doctorate Degree (Phys.-Math.), ORCID ID: 0000-0003-3909-537X, WoS ResearcherID: R-3877–2016, Scopus Author ID: 7005479766, SPIN code: 2187-1380, e-mail: vla-ryabchenko@yandex.ru

SEIN, Dmitry V., senior researcher, Cand. Sc. (Phys.-Math.), ORCID ID: 0000-0002-1190-3622, WoS ResearcherID: P-6419–2018, Scopus Author ID: 6507684871, SPIN code: 9518-7196, e-mail: dmitry.sein@awi.de